Drug Design, Development and Therapy

Dovepress
Taylor & Francis Group

Open Access Full Text Article

ORIGINAL RESEARCH

Comprehensive Analysis of Metabolic Changes in Mice Exposed to Corilagin Based on GC-MS Analysis

Biao Xu[1,*], Changshui Wang[2,*], Xiaodong Zhu[2], Li Zhu[3], Guangkui Han[2], Changmeng Cui[2]

[1]Clinical Medical School, Jining Medical University, Jining, 272067, People's Republic of China; [2]Department of Neurosurgery, Affiliated Hospital of Jining Medical University, Jining Medical University, Jining, 272000, People's Republic of China; [3]Translational Pharmaceutical Laboratory, Jining No. 1 People's Hospital, Shandong First Medical University, Jining, 272000, People's Republic of China

*These authors contributed equally to this work

Correspondence: Changmeng Cui; Guangkui Han, Department of Neurosurgery, Affiliated Hospital of Jining Medical University, 89 Guhuai Road, Jining, Shandong, 272000, People's Republic of China, Tel +86 0537 2908518, Email cmcuidr1989@163.com; guangkui_han@163.com

Background: Corilagin is widely distributed in various medicinal plants. In recent years, numerous pharmacological activities of Corilagin have been reported, including anti-inflammatory, antiviral, hepatoprotective, anti-tumor, and anti-fibrosis effects. However, there is still a need for systematic metabolomics analysis to further elucidate its mechanisms of action. The aim of this study was to explore the pharmacological mechanism of Corilagin.

Methods: This study utilized gas chromatography-mass spectrometry (GC-MS) to analyze central target tissues, comprehensively exploring the pharmacological mechanism of Corilagin in mouse models. We identified the differential metabolites by multivariate analyses, which include principal component analysis (PCA) and orthogonal partial least squares discriminant analysis (OPLS-DA). Using MetaboAnalyst 5.0 and the KEGG database was used to depict the 12 key metabolic pathways.

Results: Compared with the control group, the Corilagin induced 20, 9, 11, 7, 16, 19, 14, 15, and 16 differential metabolites in the intestine, lung, kidney, stomach, heart, liver, hippocampus, cerebral cortex, and serum, respectively. And 12 key pathways involving glucose metabolism, lipid metabolism, and amino acid metabolism were identified following Corilagin treatment.

Conclusion: This research provides insight into the action mechanism of Corilagin's anti-oxidative, anti-inflammatory, anti-atherosclerotic, hepatoprotective, anti-tumor, and neuroprotective properties.

Keywords: Corilagin, gas chromatography-mass spectrometry, metabolomics, amino acids, pharmacological mechanism

Introduction

Corilagin is a type of ellagitannin that can be extracted from various medicinal plants, including *Phyllanthus emblica L, Phyllanthus niruri Linn, Phyllanthus urinaria L*. It is a gallotannin polyphenolic compound with a chemical formula of $C_{27}H_{22}O_{18}$ (beta-1-*O*-galloyl-3,6-(*R*)-hexahydroxydiphenoyl-D-glucose) and a molecular weight of 634.5 g/mol. Corilagin is an off-white acicular crystalline powder that easily dissolves in MeOH, EtOH, acetone and DMSO (Source: https://pubchem.ncbi.nlm.nih.gov/compound/73568). The pharmacological activity and mechanisms of plant extracts have been studied extensively to discover a wide range of medicines for treating various diseases.[1] In recent years, Corilagin has attracted more attention due to its numerous pharmacological activities, such as anti-oxidative, anti-inflammatory, antiatherosclerotic, hepatoprotective, anti-tumor, antiviral, and anti-fibrosis effects. However, previous studies on pharmacological mechanisms of Corilagin have primarily focused on the signaling pathways, and systematic metabolomics analysis of Corilagin's effects in mice has yet to be conducted. Therefore, it seems necessary to conduct a comprehensive evaluation of Corilagin-induced changes in mice based on metabolomics to gain a deeper understanding of its pharmacological properties and potential applications in medicine.

Received: 14 June 2024
Accepted: 14 January 2025
Published: 21 January 2025

Graphical Abstract

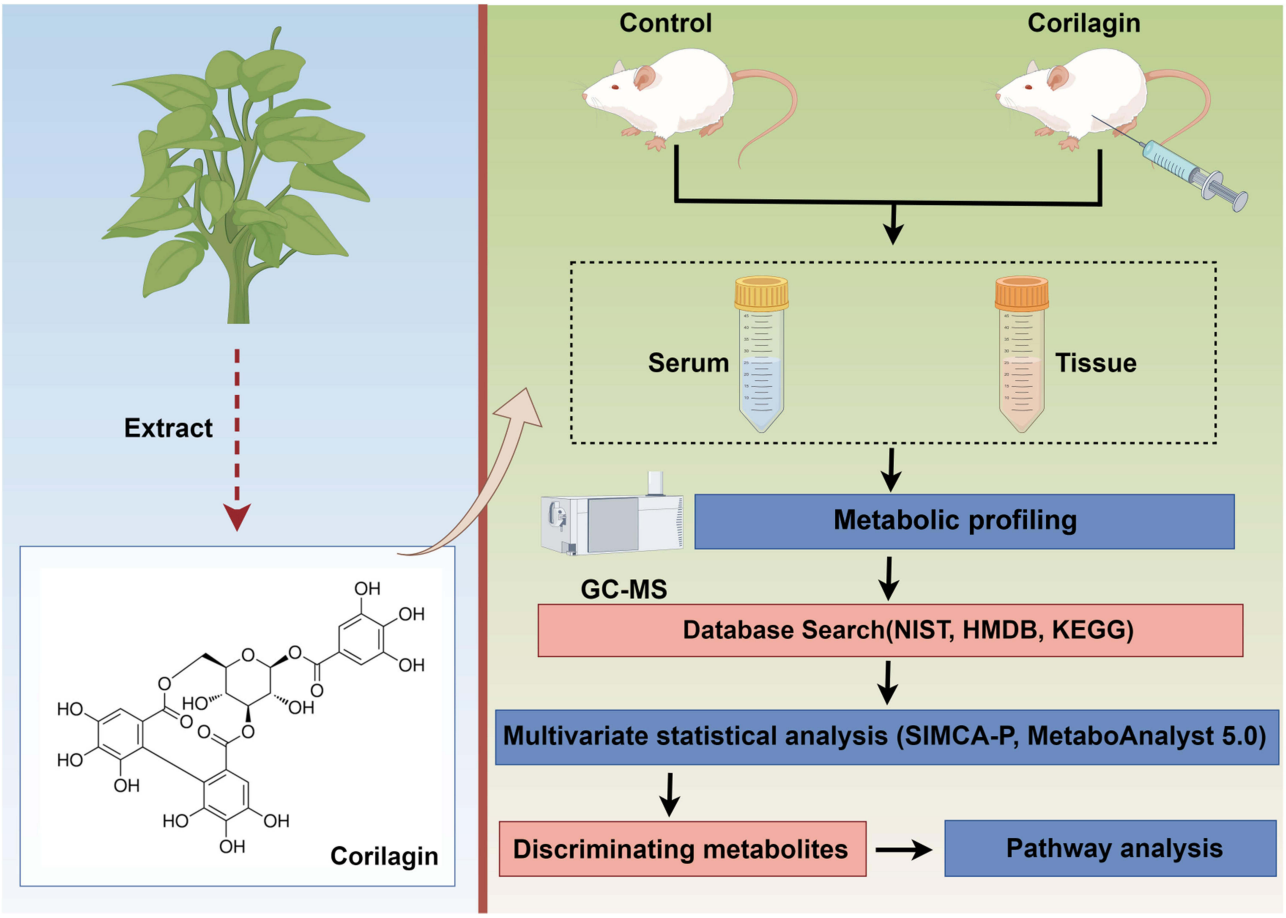

Metabolomics, a facet of systems biology, delves into the comprehensive repercussions of exogenous substances on organisms. It can reflect changes in biochemical processes and states in the body, leading to the discovery of the biochemical basis of drug action and their underlying mechanisms.[2] A study employing high-performance liquid chromatography quadrupole time-of-flight mass spectrometry to explore the metabolic processes of Corilagin's in vivo and ex vivo metabolic dynamics showed extensive Phase II metabolism in mice and the metabolic pathways involve methylation, hydrolysis, reduction, glucuronidation, sulfation and glycosylation.[3]

Yet, there are no reports of metabolomics by gas chromatography-mass spectrometry (GC-MS) method to study the pharmacological mechanism of Corilagin. We are the first study to use GC-MS to perform a comprehensive and systematic metabolomics of the effects of Corilagin on major tissues and organs – namely, intestine, lung, kidney, stomach, heart, liver, hippocampus, cortex, and serum. The advantages of GC-MS encompass remarkable stability, accurate qualitative analysis, greater separation efficiency, and high sensitivity.[4] Metabolites were identified by multivariate analyses, including principal component analysis (PCA) and orthogonal partial least squared-discriminant analysis (OPLS-DA). Furthermore, MetaboAnalyst 5.0 and KEGG database were used to define the affected metabolic pathways. Our research will reveal new insights into the pharmacological mechanism of Corilagin.

Material and Methods

Reagents

Heptadecanoic acid (purity ≥ 98%), pyridine, methanol (chromatographic grade), and Corilagin were provided by Macklin Biochemical (Shanghai, China). O-methylhydroxylamine hydrochloride (purity ≥ 98%) was procured from J&K Scientific (Beijing, China), while N, O-bis(trimethylsilyl) trifluoroacetamide (containing 1% trimethylchlorosilane) was sourced from Sigma Aldrich (St. Louis, MO, USA).

Animals and Treatment

Kunming mice weighing 30–35 g (six-week-old) were purchased from the Medical Experimental Center of Lanzhou University. Mice were acclimatized for 1 week under conditions of 20 ± 2°C with a 12-hour light/dark cycle. Determination of the Minimum Sample Size by Employing the Formula Applicable to Two Independent Groups: $n = 2 \times (Z\alpha/2 + Z\beta)^2 \times \sigma^2 / \Delta^2$, $Z\alpha/2 = 1.96$ (for $\alpha = 0.05$), $Z\beta = 0.84$ (for 80% power), σ = pooled standard deviation (based on prior studies or pilot data, estimated at 30%), Δ = minimum detectable difference between the means of the two groups (assumed to be 45%, based on biological relevance), Substituting these values into the formula: $n = 2 \times (1.96 + 0.84)^2 \times (0.3)^2 / (0.45)^2$, $n \approx 9.3$ animals per group. Thus, the mice were divided into two groups: the control group and the Corilagin group, with each group comprising ten mice, amounting to a total of twenty mice. In the Corilagin group, mice were intraperitoneally administered a daily dose of 30 mg/kg (body weight), while the control group received equivalent saline. The duration of treatment was 2 weeks. The determination of the Corilagin dosage was informed by a previously published methodology. The study conducted by Fan et al demonstrated that Corilagin (at a dosage of 30 mg/kg/day) exhibited a significant effect in inhibiting microglial cell activation and reducing the expression of inflammatory cytokines, outperforming other tested dosages.[5] Ethical approval for all experimental procedures was obtained from the Affiliated Hospital of Jining Medical University's ethical committee (Approval Number: JNMC-2022-DW-041), and the study adhered to the Guidelines for the Use of Laboratory Animals (GB/T 35892–2018).

Specimen Collection

Two weeks later, mice from both groups were euthanatized via overdose of pentobarbital sodium (80 mg/kg). The mice were subjected to eyeball enucleation, and subsequently, blood samples (with a volume of 1 mL) were gathered through retro-orbital bleeding by means of sterile capillary tubes. After centrifugation at 4°C (4000 rpm for 10 min), serum samples were harvested. Subsequently, the intestine, lung, kidney, stomach, heart, liver, hippocampus, and cortex tissues were collected, and stored at −80°C for subsequent analysis.

Preparation for Serum Samples

100 μL of serum samples were mixed with heptadecanoic acid (350 μL; dissolved in methanol), followed by centrifugation at 14,000 rpm for 15 min at 4°C. The resultant supernatant was dried under nitrogen gas at 37°C. Subsequently, the extracts were subjected to a 2-hour incubation at 70°C with O-methylhydroxylamine hydrochloride (80 μL; dissolved in pyridine) followed by an additional 1-hour incubation at 70°C with 100 μL of N, O-bis(trimethylsilyl) trifluoroacetamide (containing 1% trimethylchlorosilane). After centrifugation at 14,000 rpm for 2 min at 4 °C, the mixture was filtered through a 0.22-μm pore membrane for subsequent GC-MS analysis.

Preparation for Tissue Samples

For tissue samples, 50 mg of each tissue sample was homogenized in methanol. The tissue homogenates were mixed with heptadecanoic acid (50 μL; dissolved in methanol) and then centrifuged at 14,000 rpm for 15 min at 4 °C. Subsequently, the samples were incubated at 70 °C for 90 min with O-methylhydroxylamine hydrochloride (80 μL; dissolved in pyridine) and for 60 min with N, O-bis(trimethylsilyl) trifluoroacetamide (containing 1% trimethylchlorosilane) at the same temperature. The samples were filtered through a 0.22-μm filter. Quality control samples (QCs) were performed by pooling 10 μL of each sample within the control and Corilagin groups.

GC-MS Based Metabolomics Analysis

A 7000C mass spectrometer coupled with a 7890B GC system (equipment with HP-5MS fused silica capillary column; Agilent Technologies, USA) was used for metabolomics analysis. The samples with a split ratio of 50:1 were injected into the GC-MS apparatus. Helium served as carrier gas at a flow rate of 1 mL/min. The temperatures of injection, transfer line, and ion source were 280 °C, 250 °C, and 230 °C, respectively. Electron collision ionization was set as −70 EV, with an acquisition frequency of 20 spectra/s. MS was carried out with the aid of electrospray ionization and the mass/charge (m/z) full scan range was from 50 to 800.

Data Processing and Analysis

Data analysis was performed using Mass Hunter (Version B.07.00) from Agilent Technologies. The metabolites in this study could be categorized as Level 2 – Putatively annotated compounds.[6] Briefly, a library containing all QCs was created in this study, and at the same time, GC-MS library from the US National Institute of Standards and Technology (NIST 14) was used for the identification of the unknown metabolites. All metabolites having a similarity of more than 80% were regarded as structurally identifiable. To avoid deconvolution mistakes during automated data processing and to get rid of incorrect identifications, we manually verified each metabolite identification. To match the spectra of the metabolites in the experimental samples, we then created and employed a new spectrum library called "New Library". Finally, a data matrix including the peak index (RT-m/z pair), sample name, and associated peak area was obtained.

Multivariate analysis involving PCA and OPLS-DA was performed using SIMCA-P 14.0 (Umetrics, Sartorius Stedim Biotech) after peak area normalization. To assess the OPLS-DA models' resilience, permutation testing was done. In the course of differential metabolite analysis, we initially carried out a normality test on all the collected data. Following the Shapiro–Wilk test and the homogeneity of variance test, the data could be categorized into two groups: one was normally distributed data, which satisfied the conditions of Shapiro–Wilk test significance level (sig > 0.05) and homogeneity of variance test (sig > 0.05); the other was non-normally distributed data, encompassing all the remaining metabolites. Subsequently, for the normally distributed subset, we proceeded with a *T*-test, while for the data not conforming to the normal distribution pattern, we employed the non-parametric Wilcoxon rank-sum test to ensure the robustness and accuracy of our analytical results. Metabolites with variable importance in projection (VIP) values > 1.0 and p values < 0.05 were considered potential differentially expressed metabolites. The Heatmap clusters analysis undergoes normalization and scaling procedures. Subsequently, visualization is performed utilizing MetaboAnalyst 5.0 (http://www.metaboanalyst.ca). Ward's minimum variance was used for clustering, and the Euclidean metric was used for distance measurement. For pathway analyses, MetaboAnalyst 5.0 is employed to conduct enrichment analysis, with a bubble chart being generated as a result.

Results

Differences Among GC Total Ion Chromatograms (TICs) of QCs

As illustrated in Figure 1, it depicted the TICs of quality control from different samples. All of the TICs displayed robust signals and reliable retention time (RT) reproducibility.

Multivariate Analysis for Metabolomic Data

The results of PCA displayed that obvious differences between the Corilagin groups and the control groups were observed in intestine, lung, kidney, stomach, heart, liver, hippocampus, cortex, and serum samples (Figure 2A–E and Figure 3A–D). The OPLS-DA was further method to verify the effectiveness and predictive power of the model. As the values approach 1.0, they suggest that the model is stable and possesses dependable predictive accuracy. The detailed parameter of OPLS-DA model was listed in Table 1. Additionally, the OPLS-DA model's validity was confirmed by 200 permutation tests. As manifested in Figure 2A–E and Figure 3A–D, the intersection points between blue regression line (Q^2-point) and vertical axis were all negative values, which suggested that the OPLS-DA model was validated and further indicated the obvious differences across the Corilagin and control groups.

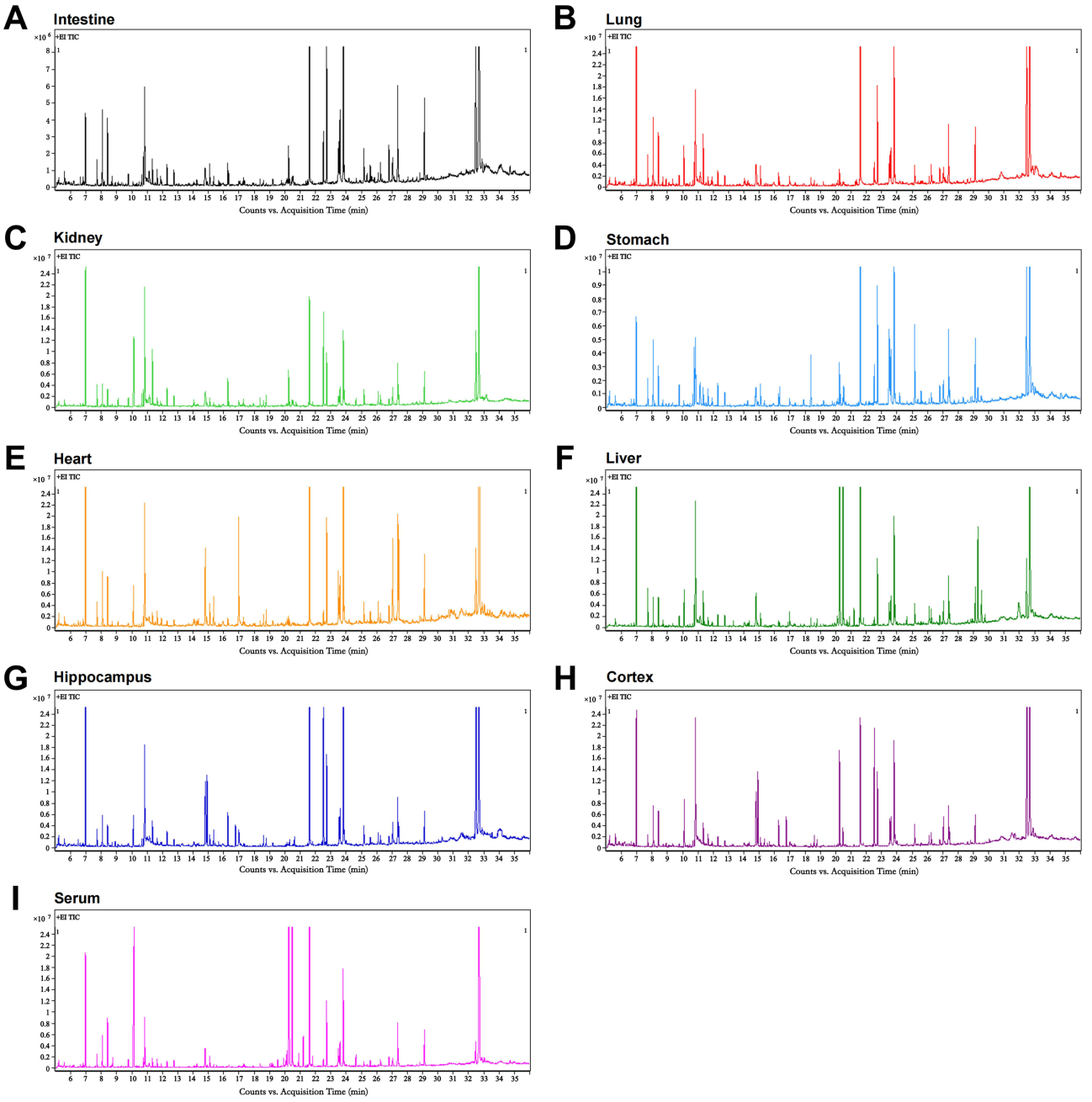

Figure 1 Representative GC–MS TICs of QCs of (**A**) intestines, (**B**) lung, (**C**) kidney, (**D**) stomach, (**E**) heart, (**F**) liver, (**G**) hippocampus, (**H**) cortex, (**I**) serum.

Identification of Metabolic Changes in Samples

The values of VIP (>1) and p (<0.05) were considered the important criteria for potential metabolites. Additionally, fold-change >1 meant that the metabolite levels showed a rising trend, while those fold-change <1 indicated a decreasing trend. A total of 64 metabolites in serum and tissues that differed significantly following the Corilagin treatment.

In the intestine, 20 differential metabolites were downregulated and included amino acids, lactic acid, fatty acids, purine derivatives, and cholesterol (Figure 4A). In the lung, a total of 9 differential metabolites (1 upregulated and 8 downregulated) were identified (Figure 4B). In the kidney, Corilagin treatment contributed to 11 altered metabolites and included 4 upregulated and 7 downregulated metabolites (Figure 4C). Meanwhile, 3 upregulated and 4 downregulated metabolites were found in the stomach (Figure 4D). Additionally, 5 upregulated metabolites and 11 downregulated metabolites in the

https://doi.org/10.2147/DDDT.S482510

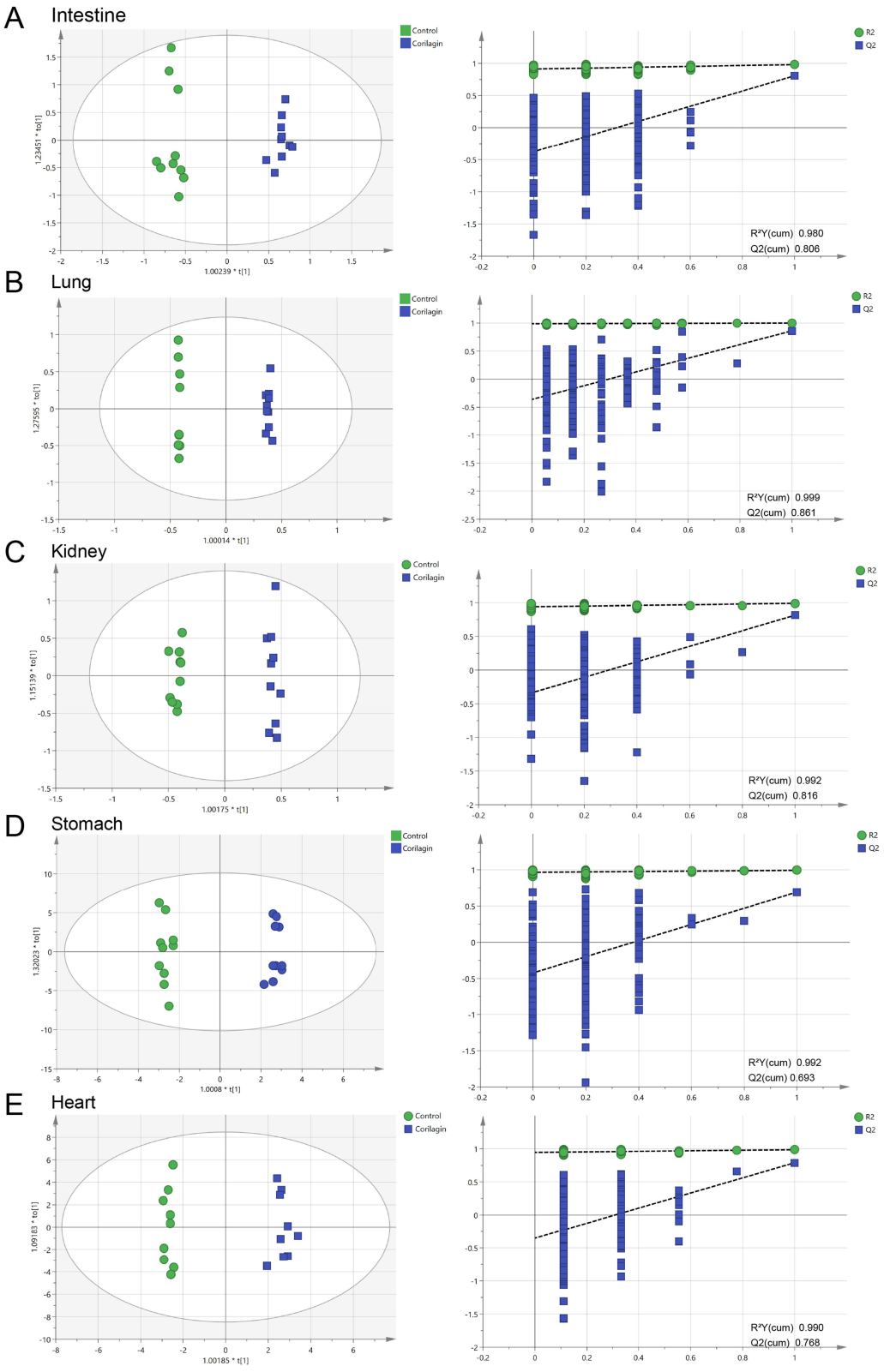

Figure 2 OPLS-DA score chart and 200 permutation tests chart. (**A**) intestines, (**B**) lung, (**C**) kidney, (**D**) stomach, (**E**) heart.

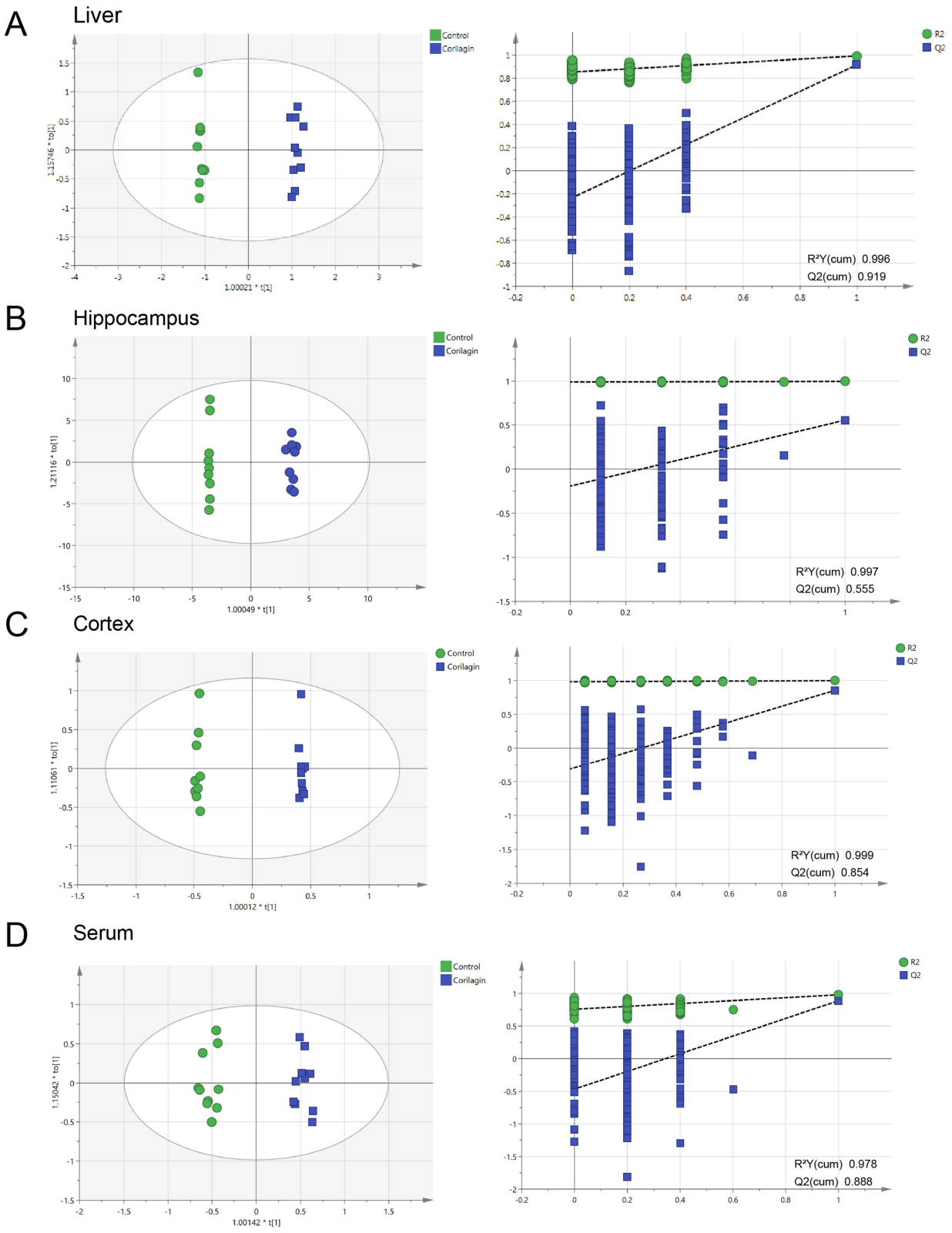

Figure 3 OPLS-DA score chart and 200 permutation tests chart. (**A**) liver, (**B**) hippocampus, (**C**) cortex, (**D**) serum.

https://doi.org/10.2147/DDDT.S482510

Table 1 OPLS-DA Parameter Scores

Tissues	R^2X (cum)	R^2Y (cum)	Q^2 (cum)
Intestine	0.445	0.980	0.806
Lung	0.559	0.999	0.861
Kidney	0.349	0.992	0.816
Stomach	0.591	0.992	0.693
Heart	0.320	0.990	0.768
Liver	0.348	0.996	0.919
Hippocampus	0.405	0.997	0.555
Cortex	0.386	0.999	0.854
Serum	0.298	0.978	0.888

heart, pyroglutamic acid, phenylalanine, inosine, myoinositol had various degrees of elevation, the levels of threonine, malic acid, methionine, arabitol, myristic acid, lysine, palmitoleic acid, palmitic acid, 1-Monopalmitin, adenosine, O-phosphoethanolamine, glycerol monostearate were decreased (Figure 4E). In the liver, 4 upregulated and 15 downregulated metabolites were found, which included succinic acid, glyceric acid, uracil, arabitol, and naphthalene levels increased in response to treatment with Corilagin. Serine, ornithine, lysine, tyrosine, gluconic acid, ribothymidine, glycerol monostearate, 9-hydroxybenzo[a]pyrene, malic acid, cysteine, arabinose, ribitol, galactose, and guanosine levels decreased after treatment with Corilagin (Figure 4F). In the hippocampus, 6 upregulated and 8 downregulated metabolites were found, including lactic acid, uracil, inosine, lactose, valine, proline increased, and serine, aspartic acid, citric acid, scyllo-inositol, docosahexaenoic acid, MG (0:0/18:0/0:0), guanosine, phenylalanine decreased (Figure 4G). In the cortex, 4 upregulated and 11 downregulated metabolites were found, including glycine, ethanolamine, glycerol, gamma-aminobutyric acid, uracil, O-Phosphoethanolamine, valine, isoleucine, aspartic acid, citric acid, tyrosine decreased, and maleic acid, glutamic acid, inosine, adenosine increased (Figure 4H). In serum, 2 upregulated and 14 downregulated metabolites were found. Glyceric acid and arachidonic acid increased in response to treatment with Corilagin, proline, threonine, methionine, glutamic acid, lysine, putrescine, tryptophan, 5-aminopentanoic acid, alanine, malic acid, DL-2-Aminooctanoic acid, ornithine, tyrosine, D-Glucose decreased significantly (Figure 4I). The more detailed results of distinct metabolites in various tissues and serum samples were displayed in Supplementary Table 1. Besides, cluster analyses of differential metabolites between the Corilagin group and the control group further validated the above results (Figure 4A–4I).

Metabolic Pathway Analysis

To further evaluate the metabolic changes in the Corilagin group compared to that of the control group, the altered metabolic pathways following Corilagin administration were identified using Metaboanalyst 5.0 (http://www.metaboanalyst.ca) and the KEGG database (http://www.kegg.jp). 12 significant pathways were identified (raw $p < 0.5$, impact > 0).

The metabolic pathways in the intestine affected are phenylalanine, tyrosine and tryptophan biosynthesis; glutathione metabolism; phenylalanine metabolism; arginine biosynthesis (Figure 5A). No significantly enriched metabolic pathways in the lung were identified (Figure 5B). Pathways in the kidney included glycerophospholipid metabolism (Figure 5C). Pathways in the stomach included galactose metabolism (Figure 5D). The metabolic pathways in the heart involved are phenylalanine, tyrosine, and tryptophan biosynthesis (Figure 5E). Pathways in the liver involved pentose phosphate pathway; glutathione metabolism; phenylalanine, tyrosine, and tryptophan biosynthesis; glycine, serine, and threonine metabolism (Figure 5F). Pathways in the hippocampus included alanine, aspartate and glutamate metabolism; phenylalanine, tyrosine and tryptophan biosynthesis (Figure 5G). Pathways in the cerebral cortex included alanine, aspartate and glutamate metabolism; glyoxylate and dicarboxylate metabolism; arginine biosynthesis; butanoate metabolism; glutathione metabolism; phenylalanine, tyrosine and tryptophan biosynthesis; glycerophospholipid metabolism (Figure 5H). The metabolic pathways in the serum involved arginine and proline metabolism; glutathione metabolism; arginine biosynthesis; alanine, aspartate and glutamate metabolism; glyoxylate

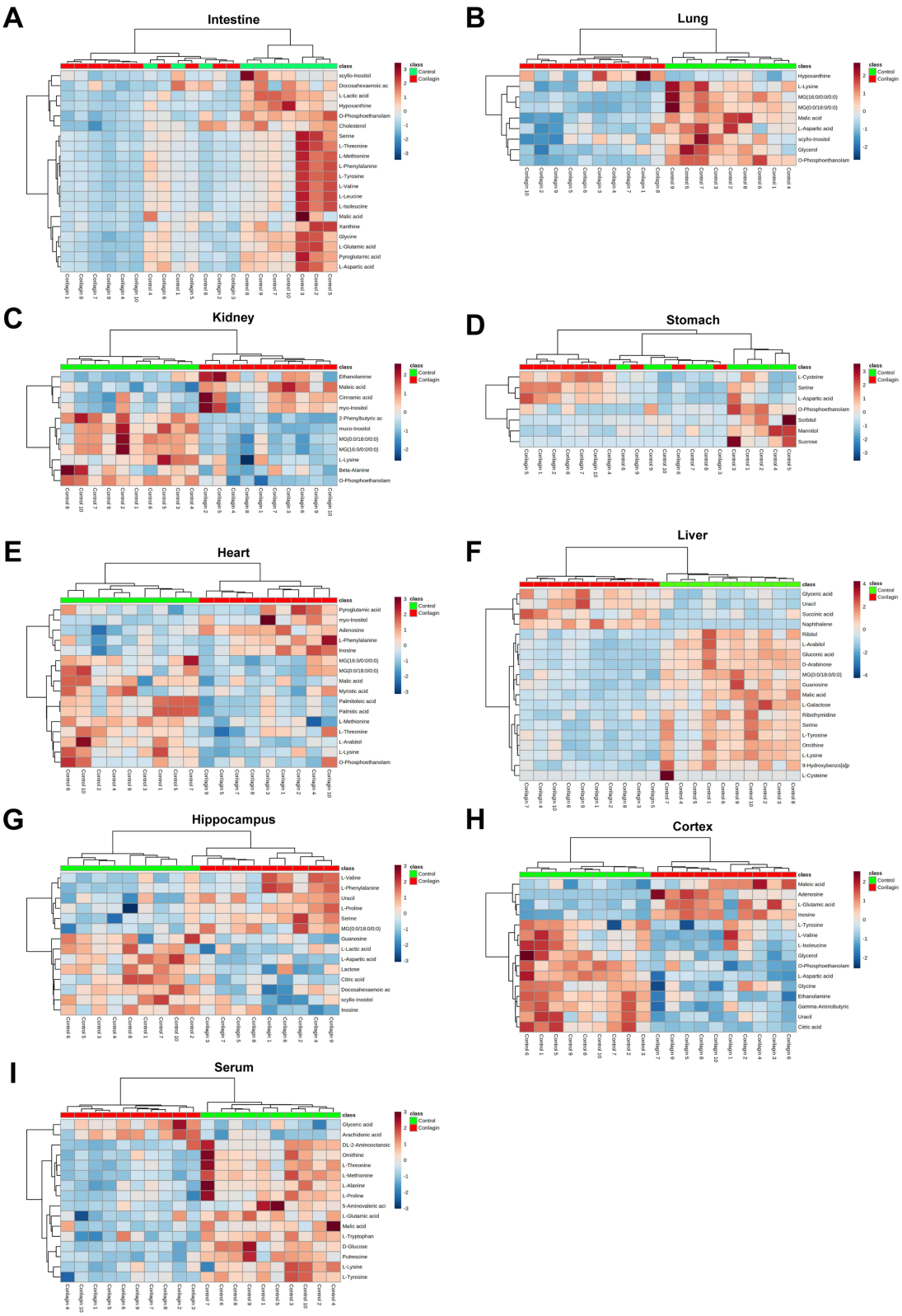

Figure 4 Heatmap of differentially expressed metabolites in (**A**) intestines, (**B**) lung, (**C**) kidney, (**D**) stomach, (**E**) heart, (**F**) liver, (**G**) hippocampus, (**H**) cortex, (**I**) serum. Samples in the Corilagin group compared to controls. The color of each part represents the importance of metabolite changes (blue, down-regulated; red, up-regulated). Columns represent metabolites, and Rows represent sample.

https://doi.org/10.2147/DDDT.S482510

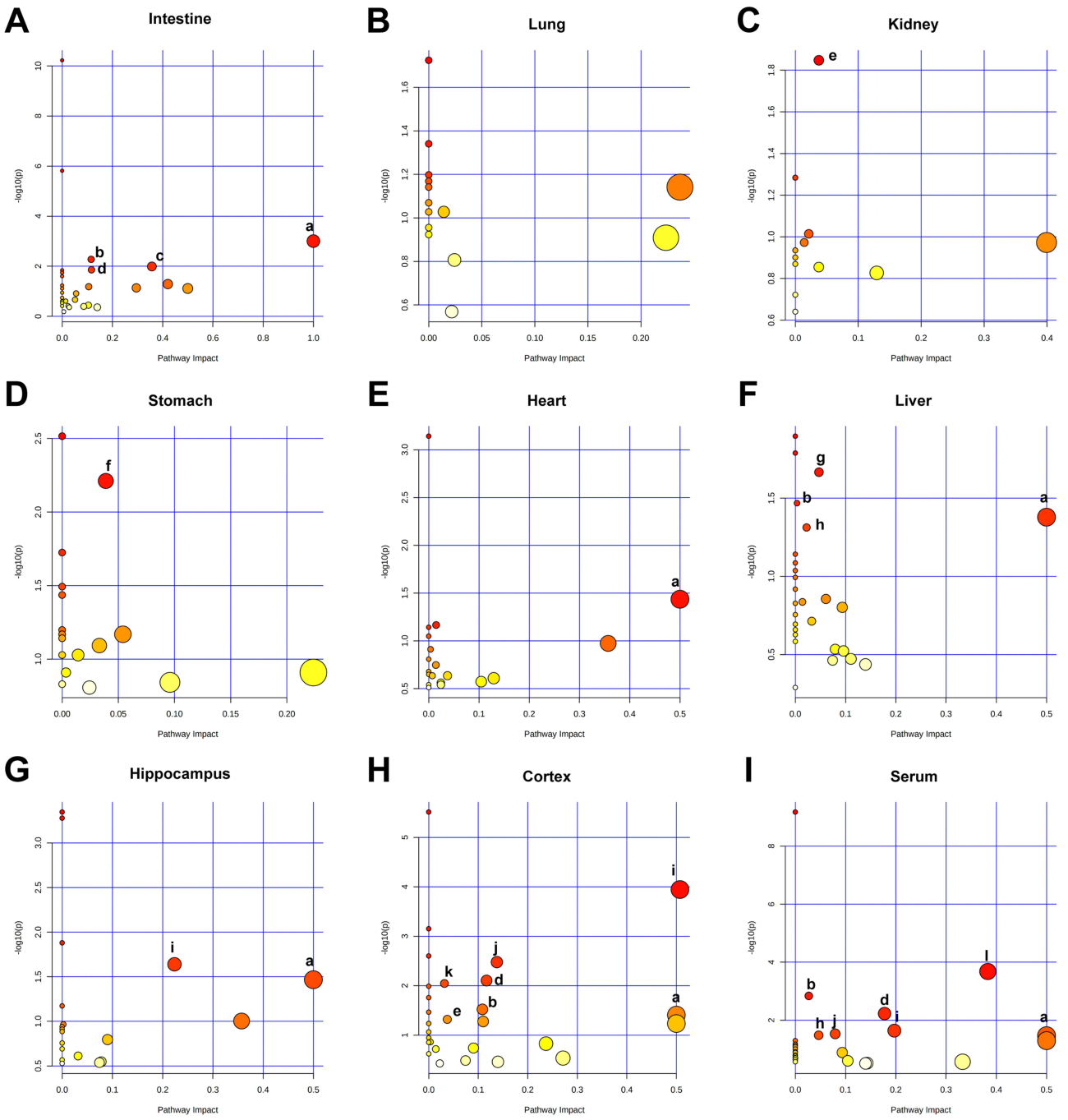

Figure 5 Pathway analysis maps were performed using MetaboAnalyst 5.0. (**A**) Pathway analysis in intestines: (**a**) Phenylalanine, tyrosine and tryptophan biosynthesis; (**b**) Glutathione metabolism; (**c**) Phenylalanine metabolism; (**d**) Arginine biosynthesis. (**B**) The related metabolic pathways enriched in the lungs. (**C**) Pathway analysis in kidney: (**e**) Glycerophospholipid metabolism. (**D**) Pathway analysis in stomach: (**f**) Galactose metabolism. (**E**) Pathway analysis in heart: (**a**) Phenylalanine, tyrosine and tryptophan biosynthesis. (**F**) Pathway analysis in liver: (**a**) Phenylalanine, tyrosine and tryptophan biosynthesis; (**b**) Glutathione metabolism; (**g**) Pentose phosphate pathway; (**h**) Glycine, serine and threonine metabolism. (**G**) Pathway analysis in hippocampus: (**a**) Phenylalanine, tyrosine and tryptophan biosynthesis; (**i**) Alanine, aspartate and glutamate metabolism. (**H**) Pathway analysis in cortex: (**a**) Phenylalanine, tyrosine and tryptophan biosynthesis; (**b**) Glutathione metabolism; (**d**) Arginine biosynthesis; (**e**) Glycerophospholipid metabolism; (**i**) Alanine, aspartate and glutamate metabolism; (**j**) Glyoxylate and dicarboxylate metabolism; (**k**) Butanoate metabolism. (**I**) Pathway analysis in serum: (**a**) Phenylalanine, tyrosine and tryptophan biosynthesis; (**b**) Glutathione metabolism; (**d**) Arginine biosynthesis; (**h**) Glycine, serine and threonine metabolism; (**i**) Alanine, aspartate and glutamate metabolism; (**j**) Glyoxylate and dicarboxylate metabolism; (**l**) Arginine and proline metabolism.

and dicarboxylate metabolism; phenylalanine, tyrosine and tryptophan biosynthesis; glycine, serine and threonine metabolism (Figure 5I). The detailed results of the pathway analysis are shown in Table 2, with a summary shown in Figure 5A–I.

 https://doi.org/10.2147/DDDT.S482510

Table 2 Metabolic Pathways Related to Corilagin Intervention Mechanisms

Pathway Name	Letter	Tissue	Match Status	Raw p	FDR	Impact
Phenylalanine, tyrosine and tryptophan biosynthesis	a	Intestine	2/4	9.90E-04	2.77E-02	1.00E+00
Glutathione metabolism	b		3/28	5.31E-03	1.12E-01	1.15E-01
Phenylalanine metabolism	c		2/12	1.02E-02	1.72E-01	3.57E-01
Arginine biosynthesis	d		2/14	1.39E-02	1.74E-01	1.17E-01
Glycerophospholipid metabolism	e	Kidney	2/36	1.42E-02	1.00E+00	3.75E-02
Galactose metabolism	f	Stomach	2/27	6.15E-03	2.58E-01	3.89E-02
Phenylalanine, tyrosine and tryptophan biosynthesis	a	Heart	1/4	3.67E-02	1.00E+00	5.00E-01
Pentose phosphate pathway	g	Liver	2/22	2.16E-02	6.05E-01	4.71E-02
Glutathione metabolism	b		2/28	3.41E-02	6.82E-01	3.43E-03
Phenylalanine, tyrosine and tryptophan biosynthesis	a		1/4	4.19E-02	6.82E-01	5.00E-01
Glycine, serine and threonine metabolism	h		2/34	4.87E-02	6.82E-01	2.25E-02
Glycerophospholipid metabolism	e		2/36	4.80E-02	2.89E-01	3.75E-02
Alanine, aspartate and glutamate metabolism	i	Hippocampus	2/28	2.29E-02	4.81E-01	2.24E-01
Phenylalanine, tyrosine and tryptophan biosynthesis	a		1/4	3.41E-02	5.73E-01	5.00E-01
Alanine, aspartate and glutamate metabolism	i	Cortex	6/48	1.14E-04	4.77E-03	5.07E-01
Glyoxylate and dicarboxylate metabolism	j		3/32	3.34E-03	5.61E-02	1.38E-01
Arginine biosynthesis	d		2/14	7.87E-03	1.08E-01	1.17E-01
Butanoate metabolism	k		2/15	9.03E-03	1.08E-01	3.18E-02
Glutathione metabolism	b		2/28	3.02E-02	2.53E-01	1.08E-01
Phenylalanine, tyrosine and tryptophan biosynthesis	a		1/4	3.93E-02	2.75E-01	5.00E-01
Arginine and proline metabolism	l	Serum	4/38	3.86E-04	1.62E-02	3.83E-01
Glutathione metabolism	b		3/28	2.26E-03	6.32E-02	2.69E-02
Arginine biosynthesis	d		2/14	7.87E-03	1.65E-01	1.78E-01
Alanine, aspartate and glutamate metabolism	i		2/28	3.02E-02	4.54E-01	1.97E-01
Glyoxylate and dicarboxylate metabolism	j		2/32	3.87E-02	4.54E-01	7.94E-02
Phenylalanine, tyrosine and tryptophan biosynthesis	a		1/14	3.93E-02	4.54E-01	5.00E-01
Glycine, serine and threonine metabolism	h		2/34	4.32E-02	4.54E-01	4.66E-02

Note: Raw p, the original p value calculated from the enrichment analysis; FDR, false discovery rate.

Discussion

Increasing evidence suggests that Corilagin exhibits anti-inflammatory, antiviral, antioxidant, hepatoprotective, antitumor, and anti-fibrotic effects. Nevertheless, there is a paucity of metabolomic investigations concerning Corilagin. Mice, a vital model organism in biomedical research, share physiological and genetic similarities with humans. Drug administration in mice can provide a critical experimental platform for simulating the drug action process and its impact on systemic metabolism. In this research, multivariate statistical analysis was utilized to investigate the influence of Corilagin on crucial organs and tissues within mice, with the aim of exploring the metabolic pathways and mechanisms of action of Corilagin. The distinctive aspect of this study is the pharmacological mechanism of Corilagin from a metabolomics perspective and the comprehensive study of metabolic alterations in mice exposed to Corilagin through GC-MS analysis.

We successfully identified 20, 9, 11, 7, 16, 19, 14, 15, 16 metabolites in the intestine, lung, kidney, stomach, heart, liver, hippocampus, cortex, and serum, respectively. These metabolites exhibited diverse fluctuations in levels, providing valuable insights into the complexity of affected metabolic pathways. Our result further revealed that the connection between the identified metabolites and 12 distinct metabolic pathways, encompassing pivotal processes such as glucose metabolism, lipid metabolism, and amino acid metabolism. The elucidation of these findings is artfully depicted in Figure 6, which visually encapsulates the Corilagin-mediated modifications in major tissue-based metabolic pathways. As a result, Corilagin exerts multifaceted therapeutic effects, encompassing anti-oxidative, anti-inflammatory, anti-atherosclerotic, hepatoprotection, antitumor responses, and neuroprotection. These remarkable outcomes are primarily orchestrated by Corilagin's intricate influence on glucose metabolism, lipid metabolism, and amino acid metabolism. To

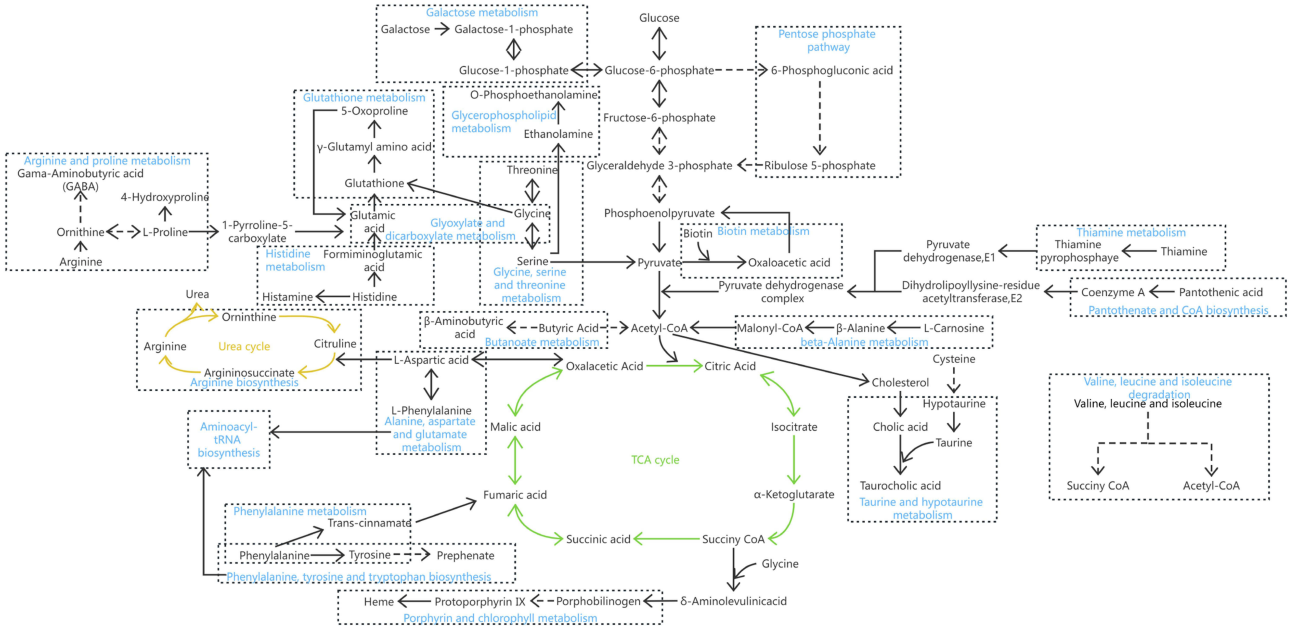

Figure 6 Schematic diagram of related metabolic pathways affected by Corilagin processing in the main tissues. Green arrows indicate the tricarboxylic acid cycle. Yellow arrows indicate urea cycle.

comprehensively expound upon the distinct pharmacological mechanism stemming from the diverse metabolic adaptations within various organs, we have discussed these alters separately below.

Brain Tissue

Oxidative stress is a major cause of neurodegenerative disorders, and oxidative processes are involved in the pathophysiology of diverse brain disorders.[7] There are two distinct antioxidant systems in the body; one is enzymatic mechanisms, including glutathione peroxidase (GSH-Px), superoxide dismutase, and catalase, and the other is non-enzymatic, mainly including glutathione, alpha-lipoic acid, vitamins, and trace elements. Glutathione, a tripeptide amalgamating glutamic acid, glycine, and cysteine, serves as a substrate for GSH-Px and glutathione S-transferase enzymes. Notably, GSH-Px can eliminate bodily peroxides, effectively impeding tissue harm caused by oxygen-derived free radicals.[8] Consequently, the amount of glutathione is an essential factor in measuring the body's antioxidant capacity. The Corilagin-treated group exhibited noteworthy elevation in glutamic acid levels, indicative of heightened production of the antioxidant glutathione. The result is consistent with the previous study by Rong Zhang,[9] which demonstrated that Corilagin could enhance the activities of GSH-Px and reduce reactive oxygen species accumulation. In addition, we observed that Corilagin affects the metabolic pathway of glutathione, which further confirms the underlying neuroprotective effect of Corilagin.

Metabolic perturbations in amino acid profiles within cerebral tissues engender a tapestry of intricate biological repercussions. Nitric oxide (NO) assumes a multifaceted role as a signaling molecule within the central nervous system, which exerts both protective and deleterious effects. A large body of accumulated evidence suggests that NO is one of the pivotal factors in the genesis of many brain-related disorders.[10] Pertinently, agents of modulating NO production, whether augmentation or inhibition, can be used as a hold promise as potential therapeutics for various neurological diseases.[10] In the Corilagin-treated group, the arginine biosynthesis pathway was affected, which in turn influencing NO generation and reduced apoptosis and necrosis of neuronal cells. In agreement with the findings of Omolara F. Yakubu, Corilagin emerges as an inhibitor of NO production.[11] N-methyl-d-aspartate receptors (NMDARs), operating as a glutamate-gated cation channel, play an important role in regulating nervous system function. Recent reports indicate distinctive compositions and signaling pathways associated with synaptic and extrasynaptic, with synaptic NMDARs tending to promote cell survival while extrasynaptic NMDARs favoring cell death. The differential activation of synaptic

and extrasynaptic yields divergent biological consequences.[12] We speculate that Corilagin could elevate in glutamate levels, thereby exerts neuroprotective effect through the activation of synaptic NMDARs.

Liver

There is a great deal of metabolic activity involving the liver. Central to hepatic functionality, the pentose phosphate pathway stood out as particularly responsive to Corilagin treatment. This pathway produces nicotinamide adenine dinucleotide phosphate, which maintains the reduced state of glutathione. Reduced glutathione is an important endogenous antioxidant, which can protect some proteins or enzymes containing sulfhydryl groups against oxidative onslaught. Notably, this antioxidant mechanism serves to impede peroxide-induced liver damage, thus buttressing hepatic resilience. Consistent with Fu-Chao Liu's study, Corilagin-treated mice showed increased glutathione levels and enhanced antioxidant capacity in the liver-injured group.[13] Evidently, Corilagin exerted a protective effect against liver injury through an antioxidant mechanism.

Hepatic biotransformation is an essential protective mechanism of the body.[14] Within this context, glucuronides capably binding to thousands of endogenous and heterologous substances, and play an important role in metabolic detoxification in vivo. Bilirubin, steroid hormones, and phenobarbital drugs undergo biotransformation by binding to glucuronides in the liver and then be excreted, in which UDP-glucuronosyltransferases (UGTs) serve as vanguards, orchestrating pivotal transformations. Within this intricate choreography, UDP glucuronosyltransferase family 2 member B4 emerges as the most abundant isoform of UGTs in adult liver.[15] Moreover, a study showed that UDP glucuronosyltransferase family 2 member B4 was increased under the intervention of Corilagin.[16] Concurrently, the Corilagin group exhibits a decrease in glucuronides. We speculate that Corilagin upregulates UGTs, thereby amplifying glucuronide metabolism. This amplification triggers the conversion of glucuronide to glucuronide, heightening hepatic detoxification prowess.

Heart

Corilagin has high pharmacological activity in the realm of cardiovascular disease treatment. Its mechanism of action includes free radicals scavenging, enhancing antioxidant enzyme activity, attenuation inflammatory factors and cyclooxygenase activity, alongside activation of the Nrf2/HO-1 signaling pathway. Increased cellular uptake of fatty acids can lead to lipid accumulation and cardiac dysfunction. Palmitic acid is the most abundant free fatty acid in food, and it is also the main inducer of lipotoxic damage. Lucas Adrian et al found that palmitic acid induces cardiomyocyte apoptosis, cytotoxic lipid accumulation and activation of the SAPK/JNK pathway.[17] The reduction of palmitic acid level induced by Corilatin provides a new perspective for the treatment of cardiac lipotoxic injury. In addition, palmitic acid has been widely reported to induce insulin resistance,[18] and palmitic acid was downregulated in the Corilagin group, which may be one of the mechanisms of Corilagin treatment of diabetes.[19]

Intestine

Central to the intricate network, branched-chain amino acids – encompassing leucine, isoleucine, and valine – reign as essential constituents for human. Elevated levels of BCAAs are strongly associated with cardiovascular disease, neurological disease, liver disease, diabetes, and cancer.[20] BCAAs trigger excessive reactive oxygen species generation and enhance autophagy-induced myocardial injury via the AMPK-ULK1 pathway.[21] Moreover, elevated plasma BCAAs can trigger arrhythmias.[22] The above evidence suggests that BCAAs increase the risk of cardiovascular disease development. Beyond the cardiovascular realm, cancer cells reside on higher energy to support their metabolism. Valeryia Mikalayeva found that up to 36% of the energy production in breast cancer cells, such as MCF-7, stems from BCAAs catabolism, thereby underscoring their pivotal role as nitrogen and carbon source for tumor cell proliferation.[23] Evidently, anti-tumor mechanism of Corilagin may be due to BCAAs curtailing tumor cell nutritional sources, thereby furnishing an anti-tumor thrust. In addition, BCAAs are involved in regulating the diversity of microbial populations in the intestine.[24] Moreover, leucine, and isoleucine biosynthesis and degradation are disturbed in the Corilagin group. This finding suggests that Corilagin as a bulwark may against the cardiovascular and diabetes, and this will further enhance the understanding of the anti-tumor mechanism of Corilagin.

Serum

Elevated homocysteine in the blood stands as an independent risk factor for the development of atherosclerosis and coronary heart disease.[25] Notably, glycine and threonine produce one-carbon units that bind to tetrahydrofolate. In the methionine cycle, this tetrahydrofolate cargo supplies methyl to homocysteine, thereby culminating in methionine synthesis. Interestingly, threonine and methionine exhibited reduced levels in the serum of Corilagin-treated mice. Hence, we hypothesize that heightened threonine metabolism potentially affords an increased abundance of one-carbon units, thus facilitating the conversion of homocysteine to methionine, thereby yielding diminished homocysteine concentrations in the serum and, correspondingly, exerting cardioprotective effects.

Arachidonic acid, a ubiquitous endogenous bioactive entity, producing prostaglandin, thromboxane, and leukotrienes.[26] Within the vascular milieu, arachidonic acid's destiny hinges upon cyclooxygenase-2 and prostacyclin synthase, ushering forth the production of prostaglandin I2 - renowned for its potent anti-platelet aggregation attributes, along with anti-inflammatory and immunosuppressive effects.[27] Noteworthy, prostaglandin D2 has anti-inflammatory and regulation of cardiovascular homeostasis effects.[28] Therefore, in the context of Corilagin, elevated serum levels of arachidonic acid may play an important role in protecting the cardiovascular system.

Conclusion

Taken together, we have conducted a systematic and comprehensive study of the pharmacological mechanism of Corilagin in terms of metabolomics. Our study showed that Corilagin affects the intricate metabolic pathways of glucose metabolism, lipid metabolism, and amino acid metabolism. These metabolomic data provide the basis for studying the mechanisms of antioxidant, anti-inflammatory, hepatoprotective, and neuroprotective effects of Corilagin. Simultaneously, the results of this study can also furnish a certain degree of reference for the clinical application of Corilagin to some extent.

Abbreviations

BCAAs, branched chain amino acids; GC-MS, gas chromatography-mass spectrometry; GSH-Px, glutathione peroxidase; m/z, mass/charge; NIST, National Institute of Standards and Technology; NMDARs, n-methyl-d-aspartate receptors; NO, nitric oxide; OPLS-DA, orthogonal partial least squared-discriminant analysis; PCA, principal component analysis; QCs, quality control samples; RT, retention time; TICs, ion chromatograms; UGTs, UDP-glucuronosyltransferases; VIP, variable importance in projection.

Data Sharing Statement

All data from the manuscript are available from the first author upon request.

Acknowldegment

The figure of the graphical was generated by Figdraw (www.figdraw.com).

CRediT Author Contributions Statement

All authors made a significant contribution to the work reported, whether that is in the conception, study design, execution, acquisition of data, analysis and interpretation, or in all these areas; took part in drafting, revising or critically reviewing the article; gave final approval of the version to be published; have agreed on the journal to which the article has been submitted; and agree to be accountable for all aspects of the work.

Funding

This study was supported by the grants from National Natural Science Foundation of China (No. 82302795), Natural Science Foundation of Shandong Province (No. ZR2023MH365, ZR2023QH094), Key Research and Development Projects of Jining City (No. 2022YXNS019). Traditional Chinese Medicine Science and Technology Project of Shandong province (No. Q-2023058). High-level Training Program of Jining Medical University (JYGC2021FKJ009).

Disclosure

The authors report no conflicts of interest in this work.

References

1. Gonulalan EM, Nemutlu E, Bayazeid O, Koçak E, Yalçın FN, Demirezer LO. Metabolomics and proteomics profiles of some medicinal plants and correlation with BDNF activity. *Phytomedicine*. 2020;74:152920. doi:10.1016/j.phymed.2019.152920
2. Kim SJ, Song HE, Lee HY, Yoo HJ. Mass Spectrometry-based Metabolomics in Translational Research. *Adv Exp Med Biol*. 2021;1310:509–531. doi:10.1007/978-981-33-6064-8_19
3. Yisimayili Z, Guo X, Liu H, et al. Metabolic profiling analysis of corilagin in vivo and in vitro using high-performance liquid chromatography quadrupole time-of-flight mass spectrometry. *J Pharm Biomed Anal*. 2019;165:251–260. doi:10.1016/j.jpba.2018.12.013
4. Abadie C, Lalande J, Tcherkez G. Exact mass GC-MS analysis: protocol, database, advantages and application to plant metabolic profiling. *Plant Cell Environ*. 2022;45(10):3171–3183. doi:10.1111/pce.14407
5. Tong F, Zhang J, Liu L, et al. Corilagin Attenuates Radiation-Induced Brain Injury in Mice. *mol Neurobiol*. 2016;53(10):6982–6996. doi:10.1007/s12035-015-9591-6
6. Viant MR, Kurland IJ, Jones MR, Dunn WB. How close are we to complete annotation of metabolomes? *Curr Opin Chem Biol*. 2017;36:64–69. doi:10.1016/j.cbpa.2017.01.001
7. Teleanu DM, Niculescu AG, Radu CI, et al. An Overview of Oxidative Stress, Neuroinflammation, and Neurodegenerative Diseases. *Int J mol Sci*. 2022;23(11). doi:10.3390/ijms23115938
8. Wang Y, Wang C, Bao S, Nie X. Responses of the Nrf2/Keap1 signaling pathway in Mugilogobius abei (M. abei) exposed to environmentally relevant concentration aspirin. *Environ Sci Pollut Res Int*. 2020;27(13):15663–15673. doi:10.1007/s11356-020-07912-3
9. Zhang R, Chu K, Zhao N, et al. Corilagin Alleviates Nonalcoholic Fatty Liver Disease in High-Fat Diet-Induced C57BL/6 Mice by Ameliorating Oxidative Stress and Restoring Autophagic Flux. *Front Pharmacol*. 2019;10:1693. doi:10.3389/fphar.2019.01693
10. Tripathi MK, Kartawy M, Amal H. The role of nitric oxide in brain disorders: autism spectrum disorder and other psychiatric, neurological, and neurodegenerative disorders. *Redox Biol*. 2020;34:101567. doi:10.1016/j.redox.2020.101567
11. Yakubu OF, Adebayo AH, Iweala EEJ, Adelani IB, Ishola TA, Zhang YJ. Anti-inflammatory and antioxidant activities of fractions and compound from Ricinodendron heudelotii (Baill). *Heliyon*. 2019;5(11):e02779. doi:10.1016/j.heliyon.2019.e02779
12. Xu J, Kurup P, Zhang Y, et al. Extrasynaptic NMDA receptors couple preferentially to excitotoxicity via calpain-mediated cleavage of STEP. *J Neurosci*. 2009;29(29):9330–9343. doi:10.1523/JNEUROSCI.2212-09.2009
13. Liu FC, Lee HC, Liao CC, Chou AH, Yu HP. Role of NADPH Oxidase-Derived ROS-Mediated IL-6/STAT3 and MAPK/NF-kappaB Signaling Pathways in Protective Effect of Corilagin against Acetaminophen-Induced Liver Injury in Mice. *Biology*. 2023;12(2). doi:10.3390/biology12020334
14. Cao YJ, Huang ZR, You SZ, et al. The Protective Effects of Ganoderic Acids from Ganoderma lucidum Fruiting Body on Alcoholic Liver Injury and Intestinal Microflora Disturbance in Mice with Excessive Alcohol Intake. *Foods*. 2022;11(7). doi:10.3390/foods11070949
15. Court MH, Zhang X, Ding X, Yee KK, Hesse LM, Finel M. Quantitative distribution of mRNAs encoding the 19 human UDP-glucuronosyltransferase enzymes in 26 adult and 3 fetal tissues. *Xenobiotica*. 2012;42(3):266–277. doi:10.3109/00498254.2011.618954
16. Yang F, Wang Y, Li G, et al. Effects of corilagin on alleviating cholestasis via farnesoid X receptor-associated pathways in vitro and in vivo. *Br J Pharmacol*. 2018;175(5):810–829. doi:10.1111/bph.14126
17. Adrian L, Lenski M, Tödter K, Heeren J, Böhm M, Laufs U. AMPK Prevents Palmitic Acid-Induced Apoptosis and Lipid Accumulation in Cardiomyocytes. *Lipids*. 2017;52(9):737–750. doi:10.1007/s11745-017-4285-7
18. Peng G, Li L, Liu Y, et al. Oleate blocks palmitate-induced abnormal lipid distribution, endoplasmic reticulum expansion and stress, and insulin resistance in skeletal muscle. *Endocrinology*. 2011;152(6):2206–2218. doi:10.1210/en.2010-1369
19. Nandini HS, Naik PR. Action of corilagin on hyperglycemia, hyperlipidemia and oxidative stress in streptozotocin-induced diabetic rats. *Chem Biol Interact*. 2019;299:186–193. doi:10.1016/j.cbi.2018.12.012
20. Yalei K, Jianyuan L, Haiying W. Branched Chain Amino Acid Metabolism and Its Relationship with Diseases. *Chin J Biochem Molecular Bio*. 2023;39(01):24–32. doi:10.13865/j.cnki.cjbmb.2022.06.1059
21. Jiang YJ, Sun SJ, Cao WX, et al. Excessive ROS production and enhanced autophagy contribute to myocardial injury induced by branched-chain amino acids: roles for the AMPK-ULK1 signaling pathway and alpha7nAChR. *Biochim Biophys Acta Mol Basis Dis*. 2021;1867(1):165980. doi:10.1016/j.bbadis.2020.165980
22. Portero V, Nicol T, Podliesna S, et al. Chronically elevated branched chain amino acid levels are pro-arrhythmic. *Cardiovasc Res*. 2022;118(7):1742–1757. doi:10.1093/cvr/cvab207
23. Mikalayeva V, Pankeviciute M, Zvikas V, Skeberdis VA, Bordel S. Contribution of branched chain amino acids to energy production and mevalonate synthesis in cancer cells. *Biochem Biophys Res Commun*. 2021;585:61–67. doi:10.1016/j.bbrc.2021.11.034
24. Dai ZL, Zhang J, Wu G, Zhu WY. Utilization of amino acids by bacteria from the pig small intestine. *Amino Acids*. 2010;39(5):1201–1215. doi:10.1007/s00726-010-0556-9
25. Esse R, Barroso M, Tavares de Almeida I, Castro R. The Contribution of Homocysteine Metabolism Disruption to Endothelial Dysfunction: state-of-the-Art. *Int J mol Sci*. 2019;20(4). doi:10.3390/ijms20040867
26. Yawei C, Jianhong L, Ning M. Research status of arachidonic acid-targeted metabonomics in inflammation. *Chin J Clin Pharmacol*. 2021;37(19):2721–2723+2728. doi:10.13699/j.cnki.1001-6821.2021.19.044
27. Dorris SL, Peebles RS Jr. PGI2 as a regulator of inflammatory diseases. *Mediators Inflamm*. 2012;2012:926968. doi:10.1155/2012/926968
28. Kong D, Yu Y. Prostaglandin D(2) signaling and cardiovascular homeostasis. *J mol Cell Cardiol*. 2022;167:97–105. doi:10.1016/j.yjmcc.2022.03.011